

Quark spin effects in e^+e^- annihilation: a Monte Carlo event generator study

A. Kerbizi^{a,*}, L. Lönnblad^{b,†} and A. Martin^{a,‡}

^a*Dipartimento di Fisica,
Università degli Studi di Trieste and INFN Sezione di Trieste,
Via Valerio 2, 34127 Trieste, Italy*

^b*Department of Physics,
Box 118, 221 00 LUND, Sweden*

(Dated: July 11, 2024)

Quark spin effects in e^+e^- annihilation to pseudoscalar and vector mesons are implemented for the first time in the PYTHIA Monte Carlo event generator. The spin-dependent fragmentation of the string stretched between the produced quark-antiquark pair with correlated spin states is described by the string- 3P_0 model implemented in the string fragmentation routine of PYTHIA by using the `StringSpinner` package. The simulated events are used to study the model predictions for the Collins asymmetries of mesons produced back-to-back in the e^+e^- center of mass system by using both the thrust axis method and the hadronic plane method. The obtained asymmetries are compared to the available data from the BELLE and BABAR experiments and the underlying Collins analysing power from the string- 3P_0 model is compared with phenomenological extractions.

Keywords: fragmentation, quark, spin, 3P_0 , string model, hadronization

I. INTRODUCTION

The e^+e^- annihilation to hadrons is a fundamental reaction to study the hadronization, the soft QCD process that converts quarks and gluons to hadrons. According to the factorization theorem [1], the e^+e^- reaction can be factorized in the elementary hard interaction $e^+e^- \rightarrow q\bar{q}$ where a quark-antiquark pair $q\bar{q}$ is produced, and the subsequent hadronization of q and \bar{q} in the final state hadrons. The hadronization is described by the fragmentation functions (FFs), which encode the dynamics behind the conversion of quarks and gluons in hadrons, and are thought to be universal. A particularly relevant FF is the Collins function $H_{1q}^{\perp h}$ that implements the Collins effect, namely the fragmentation $q^\uparrow \rightarrow h + X$ of a transversely polarized quark q into unpolarized hadrons [2]. In the annihilation reaction $e^+e^- \rightarrow h_1 h_2 X$, the Collins effect is responsible for the correlations between the azimuthal angles of the hadrons h_1 and h_2 produced back-to-back in the e^+e^- center of mass system (CMS). The strength of such correlations is quantified by the Collins asymmetry in e^+e^- , which couples the functions $H_{1q}^{\perp h}$ and $H_{1\bar{q}}^{\perp h}$. The Collins asymmetry in e^+e^- has been measured to be non-vanishing by the BELLE [3, 4], BABAR [5, 6] and BESIII [7] experiments.

In addition to being interesting by itself, the Collins FF is also needed to access the transverse polarization of quarks in a transversely polarized nucleon, encoded in the transversity parton distribution function h_1^q . This can be done by measuring the semi-inclusive deep inelastic scattering (SIDIS) process $lN \rightarrow l' h X$, where a high energy lepton l scatters off a target nucleon N and in the final

state at least one hadron h is observed besides the scattered lepton l' . If the target nucleon is transversely polarized, h_1^q is coupled with $H_{1q}^{\perp h}$ giving rise to the Collins asymmetries in SIDIS. The Collins asymmetry in SIDIS has been measured by the HERMES experiment using a proton target [8, 9], by the COMPASS experiment using a proton target [10, 11] or a deuteron target [12], and by the HALL A experiment at the JeffersonLab facility using a neutron target [13]. The asymmetry has been measured to be nonvanishing for a proton target showing that both h_1^q and $H_{1q}^{\perp h}$ are different from zero.

The Collins asymmetries in SIDIS and in e^+e^- have been used by several groups in combined phenomenological analyses aimed at extracting h_1^q and $H_{1q}^{\perp h}$ at the same time [14–18]. As a result of the analyses h_1^q and $H_{1q}^{\perp h}$ are given in terms of chosen parametrizations, the free parameters of which are obtained from fits to the Collins asymmetries in SIDIS and e^+e^- . The resulting parametrization for $H_{1q}^{\perp h}$ represents our knowledge on this FF.

An alternative approach to the phenomenological extractions using parametrizations of FFs is the modeling of the spin effects in hadronization and the implementation of the model in Monte Carlo (MC) event generators (MCEGs). Models represent our understanding of the physical mechanisms involved in hadronization, and MCEGs are needed to perform calculations that allow the comparison between the model predictions and the data. As explained in the following, work in this direction started recently. This paper, focused on the quark spin effects in e^+e^- annihilation, represents a further step forward in making realistic this alternative approach.

A recently developed model is the string- 3P_0 model, which is an extension of the Lund Model of string fragmentation [19] implemented in PYTHIA [20]. The model includes the quark spin degree of freedom at the amplitude level and was extensively studied by using standalone MC implementations [21–23]. More recently,

* albi.kerbizi@ts.infn.it

† leif.lonnblad@fysik.lu.se

‡ anna.martin@ts.infn.it

it was implemented in the hadronization part of the PYTHIA MCEG (the `StringSpinner` package [24]) for the simulation of the polarized deep inelastic scattering with production of pseudo-scalar mesons (PSMs) [25] and vector mesons (VMs) [24]. `StringSpinner` was used to carry simulations of SIDIS with a transversely polarized proton target and to study the model results for the transverse spin asymmetries like the Collins asymmetry and the dihadron asymmetries. A promising agreement with data was found [24].

In this paper we describe the first implementation of the quark spin effects in the PYTHIA 8.3 MCEG in the simulation of e^+e^- annihilation to hadrons taking into account the correlations between the spins of the intermediate $q\bar{q}$ pair. To describe the quark spin effects in the string fragmentation we use the development of the $\text{string}+^3P_0$ model for the fragmentation of a string stretched between a $q\bar{q}$ pair with correlated spin states [26]. The implementation in PYTHIA is achieved by extending the `StringSpinner` package of Ref. [24] to e^+e^- annihilation events including the spin effects for the production of final state PSMs and VMs. We use the new package to simulate e^+e^- events at the CMS energy $\sqrt{s} = 10.6 \text{ GeV}$ corresponding to the energy of the BELLE [3] and BABAR [5] experiments.

The detailed description of the implementation of e^+e^- annihilation with quark spin effects in PYTHIA is presented in Sec. II. In Sec. III we summarize the formalism of the Collins asymmetries measured in e^+e^- . The results on such asymmetries from simulated e^+e^- annihilation events are discussed in Sec. IV and compared with the results from the BELLE and BABAR experiments. In Sec. V we calculate the Collins analysing power, the ratio of $H_{1q}^{\perp h}$ and the spin-averaged FF D_{1q}^h , from the $\text{string}+^3P_0$ model and compare it with phenomenological extractions. Finally, the conclusions are given in Sec. VI.

II. IMPLEMENTATION OF THE $\text{STRING}+^3P_0$ MODEL IN PYTHIA FOR e^+e^- ANNIHILATION

In this section we describe in detail the different steps applied in `StringSpinner` to implement the quark spin effects in PYTHIA for e^+e^- annihilation to hadrons. The starting points are the `StringSpinner` package in Ref. [24] and the $\text{string}+^3P_0$ model in Ref. [26].

The simulation of e^+e^- annihilation consists of three main steps: the generation of the kinematics associated to the hard reaction $e^+e^- \rightarrow q\bar{q}$, the construction of the joint spin density matrix of the $q\bar{q}$ pair, and the hadronization $q\bar{q} \rightarrow h_1, h_2, \dots$, by fragmenting the string stretched between q and \bar{q} in the final state hadrons h_1, h_2, \dots . Gluon radiation as simulated by the final state parton shower has been switched off, since would produce strings with gluon “kinks” between the quark and anti-quark with correlated spin states, and such configurations are not yet handled by the $\text{string}+^3P_0$ model. Further final state effects such as the Bose-Einstein cor-

relations are also not included in the $\text{string}+^3P_0$ model, and have been switched off.

A. The hard reaction $e^+e^- \rightarrow q\bar{q}$

To begin the simulation, we let PYTHIA generate the hard reaction $e^+e^- \rightarrow q\bar{q}$, assuming the annihilation is mediated by a virtual photon γ^* . The flavor of the quark q is selected among the kinematically allowed flavours in proportion to the squared charges $e_q^2 / \sum_a e_a^2$. For the generation of the kinematics, the differential cross section associated to $e^+e^- \rightarrow q\bar{q}$ is used. The kinematics in the e^+e^- CMS is shown in Fig. 1a, where θ is angle between the momentum \mathbf{p}_- of e^- and the momentum \mathbf{k} of q . The momenta of e^+ and \bar{q} are indicated by $\mathbf{p}_+ = -\mathbf{p}_-$ and $\bar{\mathbf{k}} = -\mathbf{k}$, respectively.

Following Ref. [26], we define the quark helicity frame (QHF) by the set of axes $\{\hat{\mathbf{x}}_q, \hat{\mathbf{y}}_q, \hat{\mathbf{z}}_q\}$. The axes are obtained as $\hat{\mathbf{z}}_q = \mathbf{k}/|\mathbf{k}|$, $\hat{\mathbf{y}}_q = \mathbf{p}_- \times \hat{\mathbf{z}}_q / |\mathbf{p}_- \times \hat{\mathbf{z}}_q|$ and $\hat{\mathbf{x}}_q = \hat{\mathbf{y}}_q \times \hat{\mathbf{z}}_q$. The antiquark helicity frame (AHF) is defined by the axes $\{\hat{\mathbf{x}}_{\bar{q}}, \hat{\mathbf{y}}_{\bar{q}}, \hat{\mathbf{z}}_{\bar{q}}\}$, obtained analogously by using $\bar{\mathbf{k}}$ instead of \mathbf{k} . The QHF and AHF are also shown in Fig. 1. They coincide with the definitions used in Ref. [27]. In the e^+e^- CMS, the momenta of e^- and q can be expressed in the QHF as $\mathbf{p}_- = \sqrt{s}(-\sin\theta, 0, \cos\theta)/2$ and $\mathbf{k} = \sqrt{s}(0, 0, 1)/2$, where the electron and the quark masses are neglected.

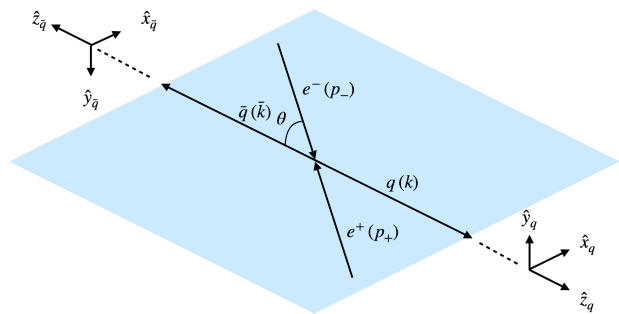


FIG. 1. Kinematics of the $e^+e^- \rightarrow q\bar{q}$ in the CMS.

B. The joint spin density matrix of $q\bar{q}$

Once the $q\bar{q}$ pair is generated, the joint spin density matrix $\rho(q, \bar{q})$ is set up. It implements the correlations between the (entangled) spin states of q and \bar{q} . Neglecting quark masses, the joint spin density matrix reads [26, 28]

$$\rho(q, \bar{q}) = \frac{1}{4} [1^q \otimes 1^{\bar{q}} - \sigma_z^q \otimes \sigma_z^{\bar{q}} + \hat{a}_{\text{NN}} (\sigma_x^q \otimes \sigma_x^{\bar{q}} + \sigma_y^q \otimes \sigma_y^{\bar{q}})], \quad (1)$$

where $\sigma_i^{q(\bar{q})}$ indicates the Pauli matrix along the axis $i = x, y, z$ in the QHF (AHF), and $1^{q(\bar{q})}$ is the identity matrix. The quantity $\hat{a}_{\text{NN}}(\theta) = \sin^2\theta/(1 + \cos^2\theta)$ describes the

correlation between the transverse spin states of q and \bar{q} originated by the tensor polarization of the γ^* .

The spin density matrices of q and \bar{q} are obtained from the joint spin density matrix as

$$\rho(q) = \text{Tr}_{\bar{q}} \rho(q, \bar{q}), \quad \rho(\bar{q}) = \text{Tr}_q \rho(q, \bar{q}). \quad (2)$$

Inserting Eq. (1) in Eq. (2), it is $\rho(q) = 1^q/2$ and $\rho(\bar{q}) = 1^{\bar{q}}/2$, meaning that q and \bar{q} are not separately polarized. Rather, their spin states are correlated.

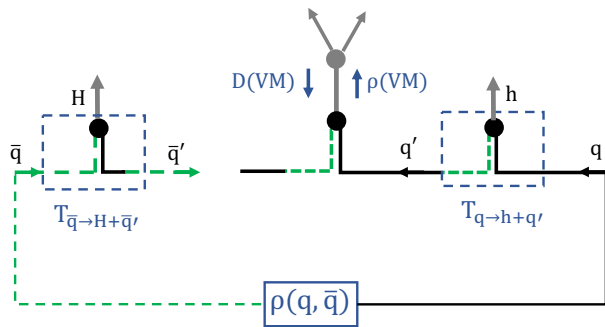


FIG. 2. Representation of the polarized string fragmentation process in **StringSpinner**.

C. The string fragmentation of the $q\bar{q}$ pair

The string fragmentation of the $q\bar{q}$ pair is simulated by PYTHIA as a recursive process of elementary quark splittings $q \rightarrow h + q'$ and elementary antiquark splittings $\bar{q} \rightarrow H + \bar{q}'$, as shown in Fig. 2. The splittings are taken from the q or the \bar{q} side randomly with equal probability.

In the quark splitting $q \rightarrow h + q'$ the emitted hadron h has four-momentum p , while the leftover quark q' has four-momentum k' . Momentum conservation yields $p = k - k'$, where k is the four-momentum of the fragmenting quark q . The transverse momenta of q , h and q' with respect to the string axis (i.e. the $q\bar{q}$ relative momentum in the CMS) are indicated by \mathbf{k}_T , \mathbf{p}_T and \mathbf{k}'_T , respectively. They are related by $\mathbf{p}_T = \mathbf{k}_T - \mathbf{k}'_T$.

In the antiquark splitting $\bar{q} \rightarrow H + \bar{q}'$, the emitted hadron H has four-momentum P while the leftover antiquark \bar{q}' has four-momentum \bar{k}' . Four-momentum conservation implies $P = \bar{k} - \bar{k}'$, where \bar{k} is the four-momentum of the fragmenting antiquark \bar{q} . The transverse momenta of \bar{q} , H and \bar{q}' with respect to the string axis are defined as $\bar{\mathbf{k}}_T$, \mathbf{P}_T and $\bar{\mathbf{k}}'_T$, respectively. They are related by $\bar{\mathbf{k}}'_T = \bar{\mathbf{k}}_T - \mathbf{P}_T$.

The h and H mesons are restricted to be PSMs and VMs, since only these are present in the string+ 3P_0 model of Ref. [26].

To implement the spin effects for an e^+e^- annihilation event, we start from the previous implementation of StringSpinner [24] and use the string+ 3P_0 model for e^+e^- annihilation in Ref. [26]. The description of the

involved steps in the simulation of e^+e^- annihilation in PYTHIA is as follows.

1. Splitting from the q side

Let us suppose the first splitting is taken from the q side. In the string+ 3P_0 model the splitting $q \rightarrow h + q'$ is described by the 2×2 splitting matrix [26]

$$T_{q',h,q} = (\dots) [\mu + \sigma_z^q \sigma^q \cdot \mathbf{k}'_T] \times \Gamma(h). \quad (3)$$

The dots indicate the scalar term of the splitting amplitude describing the energy-momentum sharing between h and q' , already implemented in PYTHIA. The quantity $\mu = \text{Re}(\mu) + i \text{Im}(\mu)$ is the complex free parameter called ‘‘complex mass’’, accounting for the 3P_0 state of quark-antiquark pairs produced at the string breakups. The vector $\sigma^q = (\sigma_x^q, \sigma_y^q, \sigma_z^q)$ is the vector of Pauli matrices in the QHF. The matrix $\Gamma(h)$ describes the coupling of q and q' with h . It is $\Gamma(h) = \sigma_z^q$ for $h = \text{PSM}$, and $\Gamma(h) = G_T \sigma^q \sigma_z^q \cdot \mathbf{V}_T^* + 1^q G_L V_L^*$ for $h = \text{VM}$. The vector $\mathbf{V} = (\mathbf{V}_T, V_L)$ is the linear polarization of the VM in the QHF. The free parameters G_T and G_L describe the coupling of q and q' with a transversely and a longitudinally polarized VM, respectively.

To introduce the spin effects in the splitting $q \rightarrow h + q'$ according to the string+ 3P_0 model, the hadron h emitted by PYTHIA is rejected if it is not a PSM or a VM. A new one is thus generated by PYTHIA, which is accepted with the probability

$$\begin{aligned} w_h(\mathbf{k}'_T; \mathbf{S}_{qT}) &= \frac{\text{Tr}_{q\bar{q}} \left[\mathbf{T}_{q',h,q}^a \rho(q, \bar{q}) \mathbf{T}_{q',h,q}^{a\dagger} \right]}{\text{Tr}_{q\bar{q}} \left[\mathbf{T}_{q',h,q}^b \mathbf{T}_{q',h,q}^{b\dagger} \right]} \\ &= \frac{1}{2} \left[1 + c \frac{2 \text{Im}(\mu)}{|\mu|^2 + \mathbf{k}'_T{}^2} \mathbf{S}_{qT} \cdot (\hat{\mathbf{z}}_q \times \mathbf{k}'_T) \right], \end{aligned} \quad (4)$$

where $\mathbf{T}_{q',h,q}^a = T_{q',h,q}^a \otimes 1^{\bar{q}}$. Here the splitting amplitude for VM emission is written as $\mathbf{T}_{q',h,q}^a = \mathbf{T}_{q',h,q}^a \mathbf{V}_a^*$, with $a = \hat{\mathbf{x}}_q, \hat{\mathbf{y}}_q, \hat{\mathbf{z}}_q$ labelling the linear polarization state of the VM in the QHF. A summation over the repeated indices is understood. If $h = \text{PSM}$, the indices a, b are omitted. w_h can be interpreted as the ratio between the probabilities for a polarized and an unpolarized splitting $q \rightarrow h + q'$ in the string+ 3P_0 model.

The second line in Eq. (4) is obtained by using the expression for the splitting matrix in Eq. (3). The effect of w_h is to introduce correlations between the transverse momentum \mathbf{p}_T of h and the transverse polarization \mathbf{S}_{qT} of q , namely the transverse part of $\mathbf{S}_q = \text{Tr} \sigma^q \rho(q)$ [see Eq. (2)]. It thus changes the azimuthal distribution of h produced by PYTHIA to emulate the spin effects of the string+ 3P_0 model and, for a non-zero \mathbf{S}_{qT} , it is responsible for the Collins effect in the emission of h . The factor c is -1 for a PSM and $f_L = |G_L|^2 / (2|G_T|^2 + |G_L|^2)$ for a VM, and governs the relative sign of the Collins effect for PSM and VM emissions. The parameter f_L describes the fraction of longitudinally polarized VMs.

Equation (4) is the analogue of the probability introduced in Refs. [24, 25] for the description of the spin effects in the DIS process.

2. Decay of vector mesons

If h is a PSM, it does not carry spin information and the decay is handled by PYTHIA. If h is a VM, its decay is instead handled by **StringSpinner**. In this case the spin density matrix of the VM is used for the simulation of the decay process. The (not normalized) spin density matrix reads [26]

$$\rho_{aa'}(h) \propto \text{Tr}_{q\bar{q}} \left[\mathbf{T}_{q',h,q}^a \rho(q, \bar{q}) \mathbf{T}_{q',h,q}^{a'\dagger} \right]. \quad (5)$$

The angular distribution of the decay products in the rest frame of the VM is generated according to $dN(p \rightarrow p_1, p_2, \dots)/d\Phi(p_1, p_2, \dots) \propto \rho_{aa'} \hat{M}_a(p \rightarrow p_1, p_2, \dots) \hat{M}_{a'}(p \rightarrow p_1, p_2, \dots)$, where $\hat{M}_a(p \rightarrow p_1, p_2, \dots)$ is the amplitude describing the decay of a VM with linear polarization a in the daughters d_1, d_2, \dots , and $d\Phi(p_1, p_2, \dots)$ indicates the relevant differential phase space factor.

The decay of h returns the decay matrix $D_{a'a} = \hat{M}_{a'} \hat{M}_a$ [26]. This matrix is required by the Collins-Knowles recipe [29, 30] to propagate the information on the orientation of the decay hadrons to the leftover quark q' , as schematically shown in Fig. 2.

3. Propagation of the spin correlations

The spin correlations are propagated by calculating the joint spin density matrix $\rho(q', \bar{q})$ of the remaining $q'\bar{q}$ pair. The (not-normalized) spin density matrix is given by [26]

$$\rho(q', \bar{q}) \propto \mathbf{T}_{q',h,q}^a \rho(q, \bar{q}) \mathbf{T}_{q',h,q}^{a'\dagger} D_{a'a}. \quad (6)$$

For a VM emission the decay matrix $D_{a'a}$ is required, while for a PSM emission the indices a and a' , and $D_{a'a}$ are removed. The matrix $\rho(q', \bar{q})$ now contains the information on the emission of h from the quark side.

4. Splitting from the \bar{q} side

After the first splitting, the next one is taken by PYTHIA randomly either from the q' side or the \bar{q} side, with equal probability. Let us suppose it is $\bar{q} \rightarrow H + \bar{q}'$ from the \bar{q} side. The procedure for implementing the spin effects is analogous to that of the q side.

The spin-dependent antiquark splitting is described in the string+ 3P_0 model by the splitting amplitude $\mathbf{T}_{\bar{q}',H,\bar{q}} = 1^q \otimes T_{\bar{q}',H,\bar{q}}$, where [26]

$$T_{\bar{q}',H,\bar{q}} = (\dots) \left[\mu + \sigma_z^{\bar{q}} \boldsymbol{\sigma}^{\bar{q}} \cdot \bar{\mathbf{k}}_{\text{T}}' \right] \times \Gamma(H). \quad (7)$$

The meaning of the different terms composing $T_{\bar{q}',H,\bar{q}}$ is analogous to those in Eq. (3), with the difference that the Pauli matrices $\boldsymbol{\sigma}^{\bar{q}} = (\sigma_x^{\bar{q}}, \sigma_y^{\bar{q}}, \sigma_z^{\bar{q}})$, the transverse momentum $\bar{\mathbf{k}}_{\text{T}}'$ as well as the polarization vector entering $\Gamma(H)$ for $H = \text{VM}$ are expressed in the AHF.

To introduce the spin effects in the splitting $\bar{q} \rightarrow H + \bar{q}'$, the hadron H generated by PYTHIA is rejected if it is not a PSM or a VM, and a new one is generated by PYTHIA still from the \bar{q} side of the string. The latter is accepted with probability

$$\begin{aligned} w_H(\bar{\mathbf{k}}_{\text{T}}'; \mathbf{S}_{\bar{q}\text{T}}) &= \frac{\text{Tr}_{q'\bar{q}} \left[\mathbf{T}_{\bar{q}',H,\bar{q}}^a \rho(q', \bar{q}) \mathbf{T}_{\bar{q}',H,\bar{q}}^{a\dagger} \right]}{\text{Tr}_{q'\bar{q}} \left[\mathbf{T}_{\bar{q}',H,\bar{q}}^b \mathbf{T}_{\bar{q}',H,\bar{q}}^{b\dagger} \right]} \quad (8) \\ &= \frac{1}{2} \left[1 + c \frac{2 \text{Im}(\mu)}{|\mu|^2 + \bar{\mathbf{k}}_{\text{T}}'^2} \mathbf{S}_{\bar{q}\text{T}} \cdot (\hat{\mathbf{z}}_{\bar{q}} \times \bar{\mathbf{k}}_{\text{T}}') \right], \end{aligned}$$

where the second line is obtained by using Eq. (7).

w_H introduces a modulation in the azimuthal distribution of the transverse momentum \mathbf{P}_{T} of H expressed in the AHF. The modulation depends in this case on the transverse part $\mathbf{S}_{\bar{q}\text{T}}$ of the polarization vector $\mathbf{S}_{\bar{q}} = \text{Tr} \boldsymbol{\sigma}^{\bar{q}} \rho(q', \bar{q})$ of \bar{q} . As shown in Ref. [26], after the emission of h the antiquark \bar{q} acquires a transverse polarization $\mathbf{S}_{\bar{q}\text{T}} \neq \mathbf{0}$ depending on the transverse momentum \mathbf{p}_{T}^1 . Through Eq. (8), this leads to correlations between the azimuthal angles of the transverse momenta \mathbf{p}_{T} of h and \mathbf{P}_{T} of H . w_H can therefore be interpreted as the conditional probability for emitting H from the \bar{q} side of the string once the hadron h has been emitted from the q side. In the string+ 3P_0 model, this is the mechanism for the generation of the Collins asymmetry for hadrons produced back-to-back in e^+e^- [26].

For the decay of H and the propagation of the spin information after its generation, the same steps as in Sec. II C 2 and Sec. II C 3 are employed provided that the substitutions $\mathbf{T}_{q',h,q} \rightarrow \mathbf{T}_{\bar{q}',H,\bar{q}}$ and $\rho(q, \bar{q}) \rightarrow \rho(q', \bar{q})$ are performed.

5. Exit condition.

The procedure described in the previous paragraphs is applied recursively by randomly emitting hadrons from the q and \bar{q} sides of the string, until the exit condition of the string fragmentation process is called by PYTHIA. At this step a remaining string piece $q_m \bar{q}_n$ must be fragmented by one last breaking by a $q' \bar{q}'$ pair and therefore the production of the final two hadrons $h = q_m \bar{q}'$ and $H = q' \bar{q}_n$.

¹ The same is true if first a hadron H is emitted from \bar{q} , then h is emitted from q . In this case the quark q acquires a transverse polarization $\mathbf{S}_{q\text{T}} \neq \mathbf{0}$ that depends on the transverse momentum \mathbf{P}_{T} of H .

To handle this last step, if the previous splitting was taken from the antiquark side, we treat the production of h as the splitting $q_m \rightarrow h+q'$ followed by the projection of the $q'\bar{q}_n$ state onto the hadronic state H . This leads to a reweight procedure for h as in Sec. II C 1 and to the decay according to Sec. II C 2 (H is taken to be unpolarized). If h is not accepted by this procedure, PYTHIA rejects the full fragmentation chain and starts all over again ².

Analogously, if the previous splitting was taken from the quark side, the production of H is seen as the splitting $\bar{q} \rightarrow H+\bar{q}'$ and treated following Sec. II C 4. In this case, if h is a VM, it is taken to be unpolarized.

This recipe is somewhat simplified with respect to that proposed in Ref. [26]. We checked, however, that the simulation results obtained with the two recipes do not differ to a noticeable degree. This is due to the fact that the spin information decays along the fragmentation chain, and the possible spin effects in the production of the final two hadrons are negligible.

III. THE COLLINS ASYMMETRIES IN e^+e^-

In inclusive two-hadron production in e^+e^- annihilation, $e^+e^- \rightarrow h_1 h_2 X$, two Collins asymmetries are introduced. They are based on two different methods: the thrust axis method, which leads to the asymmetry A_{12} , and the hadronic plane method, which leads to the asymmetry A_0 . The methods exploit different reference planes for the measurement of the relevant azimuthal angles and lead to different theoretical expressions for the Collins asymmetries.

A quantity used in both methods is the thrust axis, the best approximation of the $q\bar{q}$ axis that is measurable. It is defined as the normalized vector $\hat{\mathbf{n}}$ that maximises the event variable $T = \sum_j |\mathbf{P}_j \cdot \hat{\mathbf{n}}| / \sum_j |\mathbf{P}_j|$. The index j runs over the final state hadrons, and \mathbf{P}_j is the momentum of the hadron h_j in the CMS. T is referred to as the thrust, and it is $T \leq 1$. $T \simeq 1$ indicates a two-jet like configuration, while $T \simeq 0.5$ indicates that the distribution of the produced hadrons is roughly spherical. In experimental analyses, the two-jet like events are selected by requiring $T > 0.8$ [3, 5].

The thrust axis $\hat{\mathbf{n}}$ is used to select the back-to-back hadrons h_1 and h_2 forming a pair produced in the same event, by requiring $(\mathbf{P}_1 \cdot \hat{\mathbf{n}})(\mathbf{P}_2 \cdot \hat{\mathbf{n}}) < 0$. To reduce the association of hadrons to the wrong hemisphere, the selection $Q_T < 3.5 \text{ GeV}/c$ is applied. Q_T is the magnitude of the photon transverse momentum evaluated in the rest frame of the $h_1 h_2$ pair [3, 31]. The requirements on the

thrust and the photon transverse momentum are a common feature of the analyses performed by the BELLE [3, 4] and BABAR [5, 6] collaborations. We apply them in this paper as well.

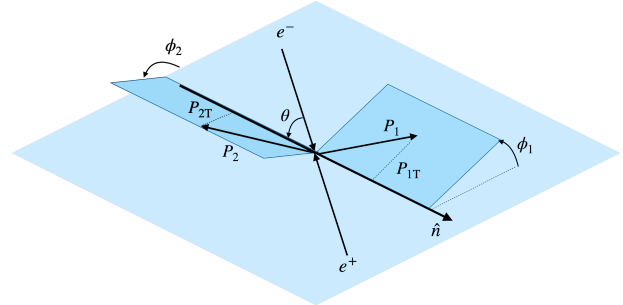


FIG. 3. The kinematics associated to the thrust axis method.

1. The A_{12} asymmetry

For the evaluation of the A_{12} asymmetry, a reference plane containing the momentum \mathbf{p}_- of the beam e^- and the thrust axis $\hat{\mathbf{n}}$ is used to measure the azimuthal angles in the CMS. As shown in Fig. 3, the transverse momentum of h_i with respect to $\hat{\mathbf{n}}$ is indicated by \mathbf{P}_{iT} and the corresponding azimuthal angle is indicated by ϕ_i , where $i = 1, 2$.

The distribution of the azimuthal angle $\phi_{12} = \phi_1 + \phi_2$ is then considered. It is expected to be (see, e.g., Ref. [14, 27, 32])

$$N_{12}(\phi_{12}; z_1, z_2, P_{1T}, P_{2T}) \propto 1 + \frac{\langle \sin^2 \theta \rangle}{\langle 1 + \cos^2 \theta \rangle} A_{12}(z_1, z_2, P_{1T}, P_{2T}) \cos \phi_{12}, \quad (9)$$

where the fractional energy of h_i is defined as $z_i = 2E_i/\sqrt{s}$, with E_i the energy of h_i . The amplitude A_{12} depends on the fractional energies z_1, z_2 and on the transverse momenta P_{1T} and P_{2T} . The dependence of A_{12} on the hard scale $Q^2 = s$ is omitted in Eq. (9). The partonic expression of A_{12} reads

$$A_{12} = \frac{\sum_{q,\bar{q}} e_q^2 \frac{P_{1T}}{z_1 m_{h_1}} H_{1q}^{\perp h_1} \frac{P_{2T}}{z_2 m_{h_2}} H_{1\bar{q}}^{\perp h_2}}{\sum_{q\bar{q}} e_q^2 D_{1q}^{h_1} D_{1\bar{q}}^{h_2}}, \quad (10)$$

where e_q is the charge of q in units of the elementary charge and m_{h_i} is the mass of hadron h_i . The numerator in Eq. (10) involves the product of two Collins FFs $H_{1q}^{\perp h_1}(z_1, P_{1T})$ and $H_{1\bar{q}}^{\perp h_2}(z_2, P_{2T})$ describing the fragmentations of transversely polarized q and \bar{q} , respectively. The summation over the flavors and antiflavors expresses the fact that each hadron can be either produced in the fragmentation of q or of \bar{q} . The denominator in Eq. (10) is given by the product of the spin-averaged FFs $D_{1q}^{h_1}(z_1, P_{1T})$ and $D_{1\bar{q}}^{h_2}(z_2, P_{2T})$, which describe the fragmentations of the unpolarized q and \bar{q} .

² This is a feature of the standard PYTHIA. By changing the code manually in such a way that only the final two hadrons are rejected, we checked that the simulation results do not differ to a noticeable degree. A gain in the execution time of the simulations is however observed.

The asymmetry A_{12} is not the directly measured quantity. To eliminate systematic effects originated by false asymmetries, the angular distribution in Eq. (9) is used to construct the normalized yields $R_{12}(\phi_{12}) = N_{12}(\phi_{12})/\langle N_{12} \rangle$ in a chosen kinematic bin, where $\langle N_{12} \rangle$ is the average yield in that bin. The ratios R_{12}^U , R_{12}^L and R_{12}^C are evaluated using unlike-sign (U) and like-sign (L) pairs, while (C) use any pair of charged hadrons. Finally the ratios

$$R_{12}^{UL(UC)} = \frac{R_{12}^U}{R_{12}^{L(C)}} \simeq 1 + \frac{\langle \sin^2 \theta \rangle}{\langle 1 + \cos^2 \theta \rangle} A_{12}^{UL(UC)} \cos \phi_{12},$$

are used to measure the amplitudes $A_{12}^{UL(UC)}$. They are given by

$$A_{12}^{UL(UC)} \simeq A_{12}^U - A_{12}^{L(C)}, \quad (12)$$

that is by the difference between the Collins asymmetry in Eq. (10) for unlike sign hadrons (A_{12}^U) and the asymmetry for like sign (A_{12}^L) or charged (A_{12}^C) hadrons.

Note that in Eq. (11) we use the convention that the factor $\langle \sin^2 \theta \rangle / \langle 1 + \cos^2 \theta \rangle$ is not included in the definition of $A_{12}^{UL(UC)}$, at variance with the definition employed experimentally [3–6].

2. The A_0 asymmetry

To evaluate the asymmetry A_0 , the plane containing the momentum \mathbf{p}_- of e^- and the momentum \mathbf{P}_2 of h_2 is considered, as shown in Fig. 4. The plane is used to measure the azimuthal angle ϕ_0 of the transverse momentum P_{0T} of h_1 with respect to \mathbf{P}_2 .

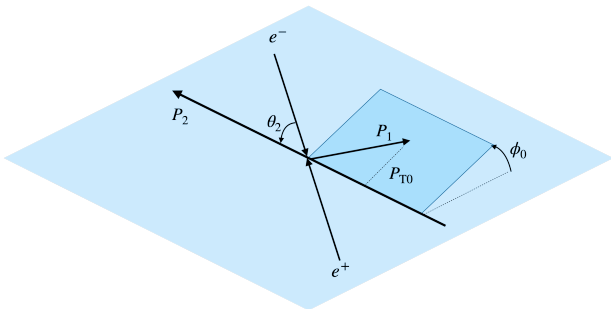


FIG. 4. The kinematics associated to the hadronic plane method.

The distribution of the azimuthal angle ϕ_0 of h_1 is expected to be [14, 27, 31, 32]

$$N_0(\phi_0; z_1, z_2, P_{0T}) \propto 1 + \frac{\langle \sin^2 \theta_2 \rangle}{\langle 1 + \cos^2 \theta_2 \rangle} A_0(z_1, z_2, P_{0T}) \cos 2\phi_0, \quad (13)$$

where θ_2 is the angle between \mathbf{P}_2 and the beam \mathbf{p}_- . The amplitude A_0 depends on z_1 , z_2 , P_{0T} and Q_T [31]. The

latter dependence is not explicitly shown. The partonic expression of A_0 is [31, 32]

$$A_0 = \frac{\sum_{q,\bar{q}} e_q^2 \mathcal{C} \left[w H_{1q}^\perp h_1 H_{1\bar{q}}^\perp h_2 \right]}{\sum_{q,\bar{q}} e_q^2 \mathcal{C} \left[D_{1q}^{h_1} D_{1\bar{q}}^{h_2} \right]}. \quad (14)$$

At variance with the A_{12} asymmetry in Eq. (10), A_0 is given in terms of the convolution of FFs over the involved transverse momenta. The convolution integral \mathcal{C} is defined as

$$(11) \mathcal{C} [w H_1 H_2] = \int d^2 \boldsymbol{\kappa}_{1T} d^2 \boldsymbol{\kappa}_{2T} \delta^{(2)}(\boldsymbol{\kappa}_{1T} + \boldsymbol{\kappa}_{2T} - \mathbf{q}_T) \times w(\boldsymbol{\kappa}_{1T}, \boldsymbol{\kappa}_{2T}) H_1(z_1, \boldsymbol{\kappa}_{1T}^2) H_2(z_2, \boldsymbol{\kappa}_{2T}^2) \quad (15)$$

for two generic FFs $H_{1,2}$ and weight factor w . The weight w appearing in the numerator in Eq. (14) can be written as $w(\boldsymbol{\kappa}_{1T}, \boldsymbol{\kappa}_{2T}) = 2 \mathbf{P}_{0T} \cdot \boldsymbol{\kappa}_{1T} \mathbf{P}_{0T} \cdot \boldsymbol{\kappa}_{2T} / P_{0T}^2 - \boldsymbol{\kappa}_{1T} \cdot \boldsymbol{\kappa}_{2T}$. The integral is performed over the transverse momenta $\boldsymbol{\kappa}_{1T}$ of q and $\boldsymbol{\kappa}_{2T}$ of \bar{q} in the rest frame of the pair $h_1 h_2$. Transverse momentum conservation in the photon decay to the quark pair is ensured by the δ -function, with $\mathbf{q}_T = -\mathbf{P}_{0T}/z_1$ being the photon transverse momentum in the rest frame of the $h_1 h_2$ pair.

Similarly to the A_{12} asymmetry, A_0 is measured from the ratio $R_0^{UL(UC)}$ between the normalized yields $R_0^U = N_0^U / \langle N_0^U \rangle$ for unlike sign hadrons and $R_0^{L(C)} = N_0^{L(C)} / \langle N_0^{L(C)} \rangle$ for like sign (L) or charged (C) hadrons. The ratios

$$R_0^{UL(UC)} = \frac{R_0^U}{R_0^{L(C)}} \simeq 1 + \frac{\langle \sin^2 \theta_2 \rangle}{\langle 1 + \cos^2 \theta_2 \rangle} A_0^{UL(UC)} \cos 2\phi_0, \quad (16)$$

are used to measure A_0^{UL} , the Collins asymmetry with the hadronic plane method. In terms of the asymmetry in Eq. (14), it is

$$A_0^{UL(UC)} \simeq A_0^U - A_0^{L(C)}. \quad (17)$$

Likewise to Eq. (11), $A_0^{UL(UC)}$ is given by the difference between the Collins asymmetries for unlike charged (A_0^U) and like charged (A_0^L) or charged (A_0^C) back-to-back hadron pairs.

Note that, as can be seen from Eq. (16), we use the convention that the factor $\langle \sin^2 \theta_2 \rangle / \langle 1 + \cos^2 \theta_2 \rangle$ is not included in the definition of the $A_0^{UL(UC)}$ asymmetry.

IV. THE COLLINS ASYMMETRIES FROM SIMULATED e^+e^- EVENTS

To study the quark-spin effects in e^+e^- annihilation in the string+ 3P_0 model we have evaluated both the A_{12} and A_0 Collins asymmetries following the data analysis described in the previous section.

The settings and values of the relevant parameters used in the simulations are described in Sec. IV A.

In Sec. IV B we present the results on the asymmetry A_{12} and compare them with the results of the BELLE and BABAR experiments.

The corresponding results for A_0 are given in Sec. IV C.

A. Simulation settings and validation

We generated $60 \cdot 10^6$ e^+e^- annihilation events with PYTHIA and the new **StringSpinner** package. The events have been generated at the same energy for BELLE and BABAR, namely $\sqrt{s} = 10.6$ GeV. The annihilation reaction is mediated by a virtual photon, which is allowed to decay to $q\bar{q}$ pairs with $q = u, d, s$. Thus the production of the heavier charm and bottom quarks has been switched off.

For the free parameters of the (spin-less) Lund string Model we used the default values in PYTHIA 8.3, as we did in Ref. [24]. The additional free parameters are those introduced by the $\text{string}+^3P_0$ model. For the complex mass μ we use $\text{Re}(\mu) = 0.42$ GeV/ c^2 and $\text{Im}(\mu) = 0.76$ GeV/ c^2 as in Ref. [24]. The fraction f_L of longitudinally polarized VMs with respect to the string axis is set to $f_L = 0.12$, meaning that VM production with transverse polarization with respect to the string axis is favored. The oblique polarization θ_{LT} is taken to be $\theta_{LT} = -0.65$, meaning that the interference between VMs with longitudinal and transverse polarizations with respect to the string axis is different from zero. The values of f_L and θ_{LT} differ from those used in Ref. [24], $f_L = 0.92$ and $\theta_{LT} = 0$. The values used here were selected to obtain a satisfactory agreement with the experimental results. They also give a satisfactory comparison with the Collins and dihadron asymmetries in SIDIS, which were the observables considered in Ref. [24].

B. Results on the A_{12} asymmetry

As explained in Sec. III, the A_{12} asymmetry can be measured using the thrust axis as an approximation of the $q\bar{q}$ axis. This introduces a smearing in the measured angles of the final state hadrons and in the measured asymmetries. The correction can be evaluated using a MCEG as done for the BELLE results published in 2008 [3] and the BABAR results published in 2014 and 2015 [5, 6]. The other option is not to correct for the use of the thrust axis, as in the case of the BELLE results published in 2019 [4]. Both sets of data are discussed in the following.

1. A_{12} asymmetry with thrust axis correction

Being the experimental asymmetries corrected for the use of the thrust axis, the asymmetries from the simu-

lated events have been calculated using the true $q\bar{q}$ axis. In the analysis of simulated events, the thrust axis is used only to form the pair using hadrons from opposite hemispheres and to apply the selection on T. For each simulated event we use the PYTHIA routine for the event analysis to find the thrust axis \hat{n} and to evaluate the corresponding value of the thrust T.

For each charged hadron in a given hemisphere, all possible pairs are formed using all the back-to-back charged hadrons. In each kinematical bin, the distribution of the azimuthal angle ϕ_{12} for the unlike sign pairs, like sign pairs and charged pairs is constructed. Finally, the ratios $R_{12}^{UL(UC)}$ are fitted with a fit function based on Eq. (11) and the Collins asymmetries A_{12}^{UL} and A_{12}^{UC} are extracted.

a. *Comparison with A_{12} results from BELLE.* In Fig. 5 we show the results for the asymmetries A_{12}^{UL} (full circles) and A_{12}^{UC} (full squares) for charged pions pairs obtained with **StringSpinner**. The asymmetries are given as a function of z_1 for different bins of z_2 . The binning is the same as in the BELLE analysis [3]. Each hadron is required to have $z_i > 0.2$.

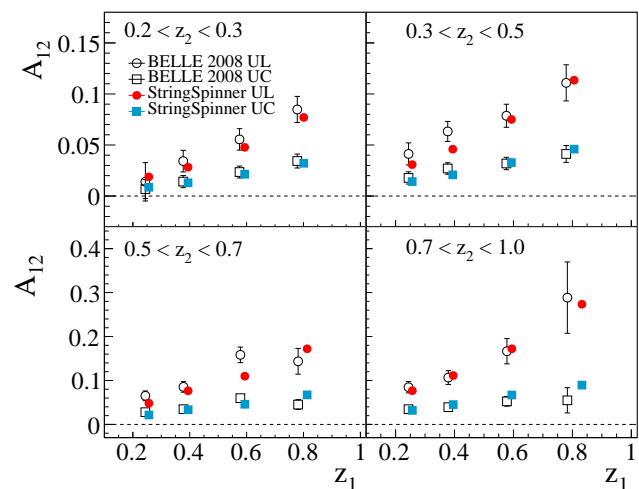


FIG. 5. Comparison between the Collins asymmetries A_{12}^{UL} and A_{12}^{UC} for back-to-back $\pi^\pm - \pi^\mp$ pairs obtained with **StringSpinner** (full markers) and the corresponding asymmetries measured by BELLE [3] (open markers).

As can be seen, the simulated asymmetries show a rising trend as a function of z_1 in each z_2 bin. Hadrons with large fractional energies are likely to be produced close to the initial quarks, where the correlations between the spin states of q and \bar{q} are strongest and the resulting Collins effect is large. As studied in detail in Refs. [21–23], the spin information in the fragmentation chain decays as long as more hadrons are produced (with small z values), resulting in a small Collins effect. Note also that the simulations reproduce smaller A_{12}^{UC} asymmetries than the A_{12}^{UL} asymmetries, as observed in the data.

To better understand how the A_{12}^{UL} and A_{12}^{UC} asymmetries arise in the $\text{string}+^3P_0$ model, in Fig. 6 we show

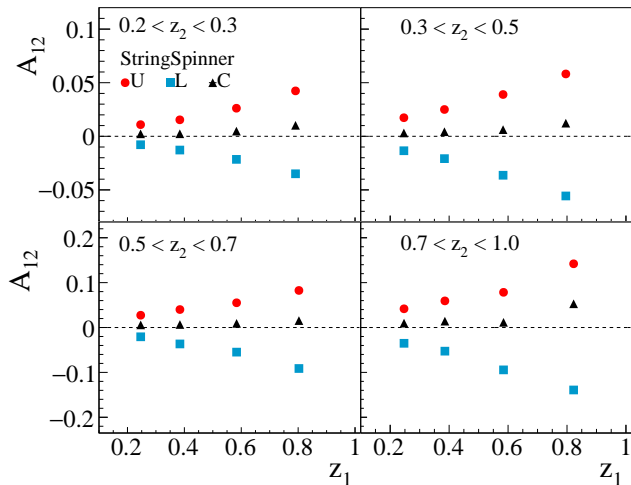


FIG. 6. The Collins asymmetries A_{12}^U (circles), A_{12}^L (squares) and A_{12}^C (triangles) for back-to-back $\pi^{\pm} - \pi^{\mp}$ pairs as obtained with **StringSpinner**. The same simulated events as for the asymmetries in Fig. 5 have been used.

separately the asymmetries A_{12}^U (circles), A_{12}^L (rectangles) and A_{12}^C (triangles). As can be seen, A_{12}^U is positive while A_{12}^L is negative. This is expected since the product of two favored Collins FFs contribute to A_{12}^U , while the product of a favored and an unfavored Collins FF appears in A_{12}^L , and in the string+ 3P_0 model the favoured and unfavored Collins FFs have opposite signs. A_{12}^C is instead close to zero due to the fact that both U and L pairs contribute, which have Collins asymmetries with opposite signs.

In Fig. 5 we also show the asymmetries A_{12}^{UL} (open circles) and A_{12}^{UC} (open squares) measured by BELLE [3]. The errorbars associated to the data correspond to the total uncertainty obtained by summing in quadrature the statistical and the systematic uncertainties. The same is done also for the data considered in the following. Note that the BELLE data are already corrected for the contribution of charm quarks [3]. Thus the comparison with the MC results is consistent. As can be seen, the comparison with data is satisfactory. The model reproduces the size and the trends of both the experimental A_{12}^{UL} and A_{12}^{UC} asymmetries.

Note that the simulated asymmetries have been slightly shifted horizontally by a constant amount to better show the comparison with data. This is done also in the following.

b. Comparison with A_{12} from BABAR. The BABAR collaboration has also measured the A_{12} asymmetries for back-to-back charged pion pairs as a function of the fractional energy z_i with a slightly different binning [6]. The asymmetries A_{12}^{UL} (open circles) and A_{12}^{UC} (open squares) measured by BABAR are shown in Fig. 7. They are corrected for the smearing effect caused by the misalignment between $\hat{\mathbf{n}}$ and the $q\bar{q}$ axis as well as for the contribution of charm quarks. The z_i

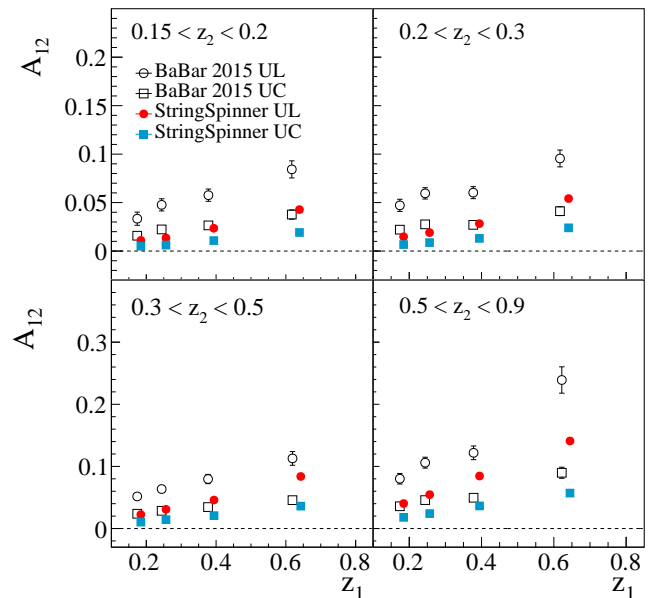


FIG. 7. The Collins asymmetries A_{12}^{UL} (full circles) and A_{12}^{UC} (full squares) for back-to-back $\pi^{\pm} - \pi^{\mp}$ pairs as obtained with **StringSpinner**, and as measured by BABAR [6] (open markers).

range has been set to $0.15 < z_i < 0.9$. In addition a cut $\alpha_i < \pi/4$ has been applied, where the opening angle α_i is the opening angle of h_i with respect to the thrust axis [6].

The closed points in Fig. 7 show the results obtained from the MC simulations as a function of the fractional energy. The trend is the same as in Fig. 5. In particular, they show a rising trend as a function of the fractional energy. The size of the asymmetries turns out to be smaller as compared to the experimental results. This is somehow expected since results from BELLE and BABAR are different, as already noted in Ref. [5].

In Fig. 8 we show the Collins asymmetries A_{12}^{UL} (full circles) and A_{12}^{UC} (full rectangles) for charged kaon pairs from MC events. The asymmetries are shown as function of z_1 for the selected bins of z_2 , and each kaon is required to have a fractional energy $0.15 < z_i < 0.9$ and an opening angle $\alpha_i < \pi/4$ as in the BABAR analysis [6]. Comparing with the A_{12} asymmetries for charged pions in Fig. 7, one can see that the string+ 3P_0 model produces a larger Collins asymmetry for kaons. To understand this feature, we recall that in the string+ 3P_0 model with only PSM production, the Collins asymmetry for the production of pions is similar to the asymmetry for the production of kaons [21]. When introducing also VM production and decay, the decay products of VMs contribute to a dilution of the Collins asymmetry of the final hadrons [23]. The dilution is less for kaons as compared to pions, due to the fact that the fraction of mesons from decays of VMs is lower in the kaon sample than in

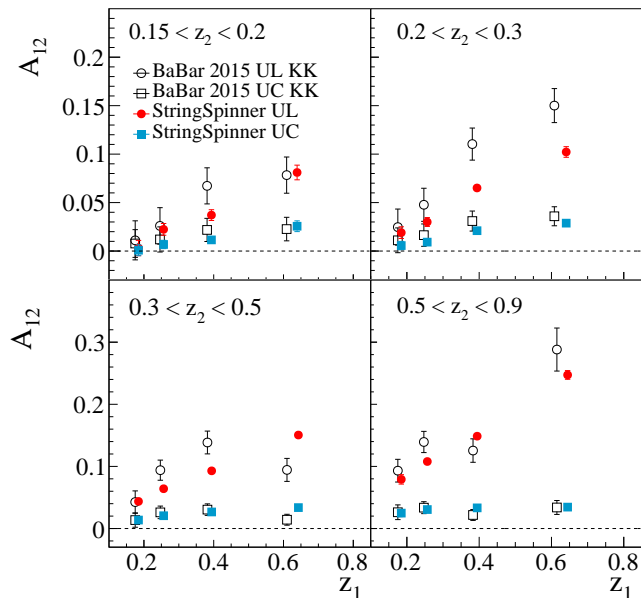


FIG. 8. The Collins asymmetries A_{12}^{UL} (full circles) and A_{12}^{UC} (full squares) for back-to-back $K^{\pm} - K^{\mp}$ pairs as obtained with **StringSpinner**, and as measured by BABAR [6] (open markers).

the pion sample.

The corresponding Collins asymmetries for charged kaons measured by BABAR are shown in Fig. 8 by the open markers. As can be seen, **StringSpinner** satisfactorily reproduces the size of the measured asymmetries for small and large z . Note that for kaon pairs the reduction of the A_{12}^{UC} asymmetries with respect to the A_{12}^{UL} asymmetries is more pronounced than in the pion case (cf. with Fig. 5), which is reproduced by the simulations.

2. A_{12} asymmetry without thrust axis correction

In this section we study the A_{12}^{UL} asymmetry evaluated using the thrust axis $\hat{\mathbf{n}}$ and not corrected for the smearing effect due to the misalignment between $\hat{\mathbf{n}}$ and the $q\bar{q}$ axis, as done for the BELLE results published in 2019 [4]. In the simulation, only the fragmentation of u , d and s quarks is allowed. The asymmetries are evaluated in the same z and P_T bins used by BELLE [4], and the same cuts $0.1 < z_i < 1.0$ and $\alpha_i < 0.3\text{rad}$ are applied. The latter cut rejects 23% of the hadron pairs. When evaluating the asymmetry as a function of the transverse momentum, each hadron is required to have $z_i > 0.2$.

The asymmetry for charged pion pairs as a function of z_1 in bins of z_2 is shown in the top plot in Fig. 9 (full circles). It exhibits a rising trend as a function of the fractional energy. The size of the asymmetry is smaller as compared to the A_{12}^{UL} asymmetry in Fig. 5 evaluated using the true $q\bar{q}$ axis. In fact, using the thrust axis

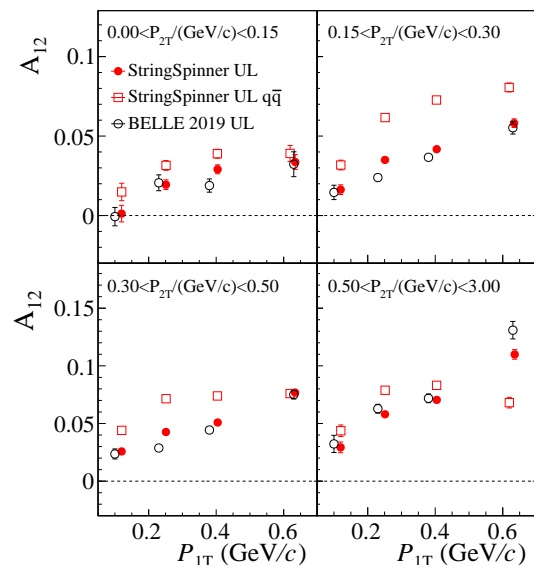
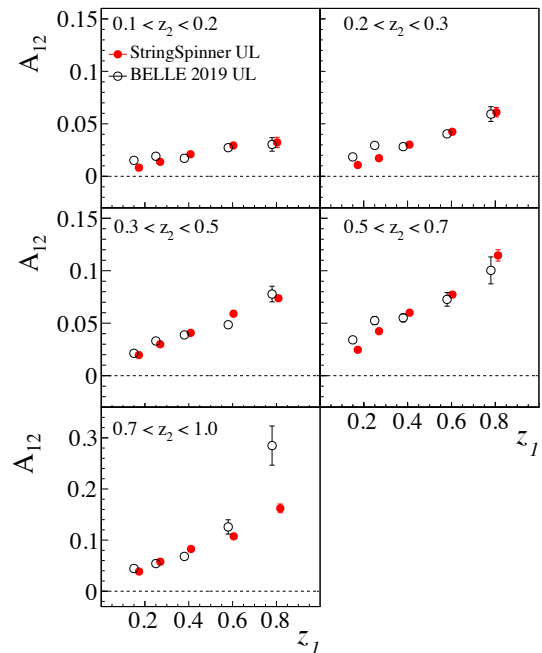


FIG. 9. The Collins asymmetry A_{12}^{UL} for back-to-back $\pi^{\pm} - \pi^{\mp}$ pairs as obtained with **StringSpinner** (full circles) and as measured by BELLE [4] (open circles). Top plot: $z_1 \times z_2$ binning. Bottom plot: $P_{1T} \times P_{2T}$ binning. The open squares represent A_{12}^{UL} evaluated by **StringSpinner** using the true $q\bar{q}$ axis.

the asymmetry is reduced by a factor of about 0.6 in agreement with the BELLE result [3].

The bottom plot in Fig. 9 shows the A_{12} asymmetry as a function of P_{1T} in bins of P_{2T} . It has nearly a linear trend in the considered transverse momentum range.

Considering that the A_{12}^{UL} asymmetry is roughly given by the product of two Collins FFs [see Eq. (10)] and the nonmonotonic P_T -dependence of the Collins analysing power for the production of pions studied by the standalone simulations in Ref. [23], one would not expect a nearly linear trend for A_{12}^{UL} as a function of transverse momentum. This can be seen by evaluating the asymmetry A_{12}^{UL} using the true $q\bar{q}$ axis, which is shown by the open squares in the same figure. Therefore, it turns out that the misalignment between the thrust axis \hat{n} and the true $q\bar{q}$ axis results in a dilution and a change of the trend of the Collins asymmetry as a function of P_T , leading to a nearly linear dependence on this variable.

The corresponding A_{12}^{UL} asymmetries measured by BELLE for back-to-back charged pion pairs are shown by the open points in Fig. 9. Unlike the 2008 BELLE results [3], these asymmetries are not corrected for the contribution of charmed quarks. To obtain the Collins asymmetries in events initiated by u , d or s quarks, we multiply the asymmetry measured by BELLE by the factor $(1 - f_c)^{-1}$, using the fraction f_c of charm-initiated events given by BELLE and assuming a vanishing Collins asymmetry resulting from such events [4].

Looking at the upper plot in Fig. 9, it can be seen that **StringSpinner** gives a satisfactory description of the experimental A_{12}^{UL} asymmetry as a function of the fractional energy. An exception is the last point for $0.7 < z_2 < 1.0$. From the bottom plot, it can be seen that simulations agree also with the magnitude and the rising trend of the Collins asymmetry as a function of transverse-momentum.

Using **StringSpinner** with the same parameter settings we evaluated also the Collins asymmetries for back-to-back $\pi^0 - \pi^\pm$ pairs and $\eta - \pi^\pm$ pairs, which were also

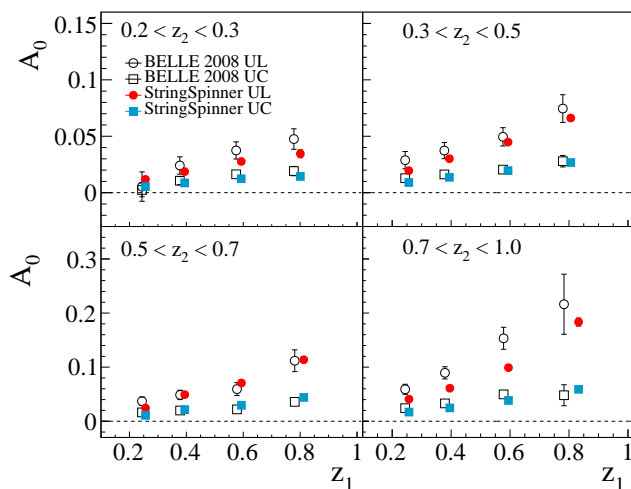


FIG. 10. The Collins asymmetries A_0^{UL} (full circles) and A_0^{UC} (full squares) for back-to-back $\pi^\pm - \pi^\mp$ pairs as obtained with **StringSpinner**, and as measured by BELLE [3] (open markers).

measured by BELLE in 2019 [4]. A description of the experimental results similar to that in Fig. 9 was found.

From the point of view of phenomenology, an analysis of the A_{12}^{UL} asymmetries measured by BELLE using the thrust axis turns out to be difficult with the presently available theoretical tools. This would require the cross section for the reaction $e^+e^- \rightarrow h_1 h_2 X$ for back-to-back hadrons h_1 and h_2 including the dependence on the thrust axis, which is not available yet. A step forward in this direction has been performed recently for the reaction $e^+e^- \rightarrow hX$, the cross section of which has been applied to the study of the transverse momentum dependence of the spin-averaged D_{1q}^h FF [33].

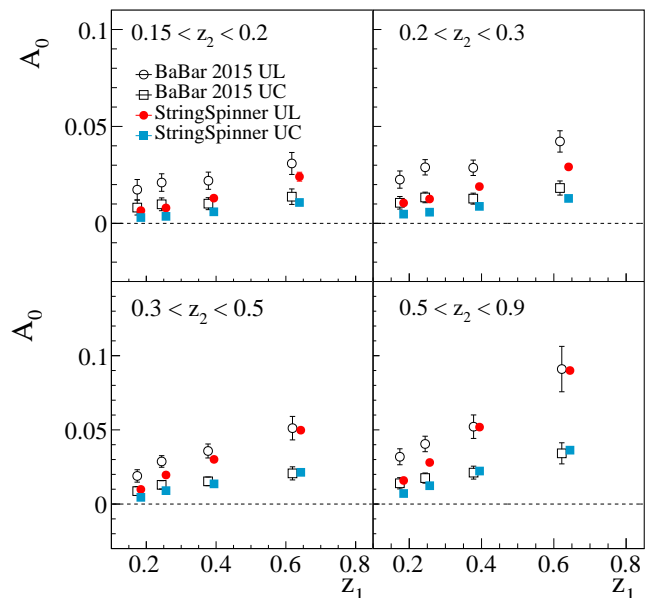


FIG. 11. The Collins asymmetries A_0^{UL} (full circles) and A_0^{UC} (full squares) for back-to-back $\pi^\pm - \pi^\mp$ pairs as obtained with **StringSpinner**, and as measured by BABAR [6] (open markers).

C. Results on the A_0 asymmetry

To calculate the Collins asymmetry A_0 we have used the same simulated events used to obtain the A_{12} asymmetry of Sec. IV B. The A_0 asymmetry has also been corrected by the experiments to account for the use of the thrust axis instead of the true $q\bar{q}$ axis. This asymmetry is however less sensitive to the misalignment between \hat{n} and the $q\bar{q}$ axis, the correction factor being about 1.10 [3, 5].

a. Comparison with the BELLE data. The results for the asymmetries A_0^{UL} (full circles) and A_0^{UC} (full rectangles) for back-to-back charged pions are shown in Fig. 10 as a function of z_1 for selected bins of z_2 . The kinematic selections and the z -binning are the same as in

the BELLE 2008 analysis in Ref. [3] (and as in Fig. 5). As can be seen, the A_0 asymmetry also exhibits a rising trend as a function of z . Comparing to the A_{12} asymmetry in Fig. 5, A_0 turns out to have lower values. This is expected because the use of the momentum of h_2 to build the hadron frame in Fig. 4 introduces a smearing analogous to the thrust axis. By comparing Fig. 10 with Fig. 9, it is interesting to note that the size of the A_0 asymmetry is similar to that of the A_{12} asymmetry without the correction for the thrust axis smearing.

The A_0 asymmetries measured by BELLE [3] are also shown in Fig. 10 (open markers). As can be seen, **StringSpinner** gives a satisfactory description of the trend as a function of the fractional energy and of the magnitude of both the A_0^{UL} and A_0^{UC} asymmetries. An exception is the interval $0.7 < z_2 < 1.0$, where the simulated results for the A_0^{UL} asymmetry is systematically lower than the BELLE data. This is not the case for the A_0^{UC} asymmetry.

b. Comparison with BABAR data. In Fig. 11, we show the simulated A_0 asymmetry (closed points) in the same two-dimensional $z_1 \times z_2$ binning as in the 2015 BABAR analysis [6]. The trend and the size of both A_0^{UL} and A_0^{UC} are similar to what obtained for BELLE in Fig. 10. This is expected since the annihilation events are carried at the same CMS energy, and that the selections applied in the analysis are similar (the cut $\alpha_i < \pi/4$ applied by BABAR rejects only the 9% of the simulated data). The corresponding Collins asymmetries measured by BABAR in 2015 are shown by the open markers in

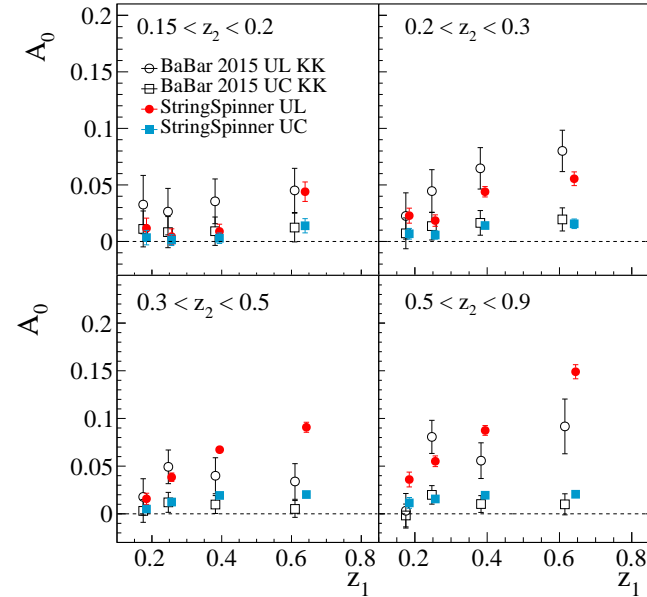


FIG. 12. The Collins asymmetries A_0^{UL} (full circles) and A_0^{UC} (full squares) for back-to-back $K^{\pm} - K^{\mp}$ pairs as obtained with **StringSpinner**, and as measured by BABAR [6] (open markers).

Fig. 11. A satisfactory description of the A_0^{UL} asymmetry is found for $z_1 > 0.3$, while if at least one of the fractional energies is less than 0.3 the simulated asymmetries are lower than the data. A similar description is also found for the A_0^{UC} asymmetry.

In Fig. 12 are shown the simulation results for the A_0^{UL} (full circles) and A_0^{UC} (full squares) asymmetries for charged kaons, in the same binning for the fractional energy as in the BABAR analysis [6]. The asymmetry has a rising trend as a function of the fractional energy and it is lower than the A_{12} asymmetry for charged kaons shown in Fig. 8. This is analogous to the A_0 asymmetry for charged pions.

The corresponding asymmetries measured by BABAR are shown in Fig. 12 by the open markers. Despite the large uncertainties in the data, the agreement between **StringSpinner** and the data is satisfactory for both the A_0^{UL} and A_0^{UC} asymmetries.

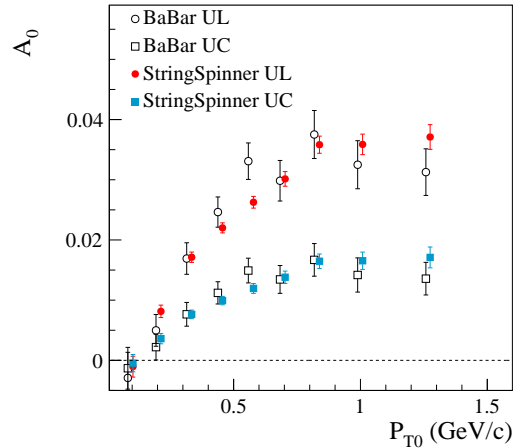


FIG. 13. Comparison between the Collins asymmetries A_0^{UL} (full circles) and A_0^{UC} (full squares) as a function of P_{0T} for back-to-back $\pi^{\pm} - \pi^{\mp}$ pairs obtained with **StringSpinner** (full markers), and the asymmetries measured by BABAR [5] (open markers).

Finally, to further investigate the transverse-momentum dependence of the A_0 asymmetry predicted by the string $^{+3}P_0$ model it is interesting to evaluate the A_0^{UL} and A_0^{UC} asymmetries for charged pion pairs as a function of P_{0T} using the simulated events. The simulation results for A_0^{UL} (closed circles) and A_0^{UC} (closed squares) are shown in Fig. 13. Both asymmetries have a peculiar transverse momentum dependence. They show a rising trend as a function of P_{0T} for $P_{0T} \leq 0.7$ GeV/c while for larger transverse momenta they flatten out. This is seen also in the corresponding BABAR results [6] shown in the same figure by the open markers. As can be seen, the agreement between the simulations and the experimental data is remarkable both for the trend and the size of the asymmetries.

This result and the satisfactory description of the transverse-momentum dependence of A_{12}^{UL} evaluated using the thrust axis in Fig. 9 (bottom), represent a test of the transverse-momentum-dependent effects in e^+e^- annihilation predicted by the string+ 3P_0 model. The reproduction of these effects is encouraging and motivates further developments of the model.

V. THE COLLINS ANALYSING POWER IN THE STRING+ 3P_0 MODEL

As can be seen from Eqs. (10) and (14) the essential ingredient of the asymmetries A_{12} and A_0 is the ratio between the Collins function $H_{1q}^{\perp h}$ and the spin-averaged FF D_{1q}^h . This ratio is related to the Collins analysing power for the fragmentation of q in h ,

$$a_p^{q^\uparrow \rightarrow h+X}(z, p_T) = \frac{p_T}{z m_h} \frac{H_{1q}^{\perp h}(z, p_T)}{D_{1q}^h(z, p_T)}, \quad (18)$$

which gives information on the nonperturbative spin-dependent dynamics involved in the hadronization process. It depends on z and the transverse momentum p_T of h with mass m_h .

The Collins analysing power is also obtained from phenomenological analyses aimed at extracting the transversity PDF and the Collins FF from the combined analysis of SIDIS and e^+e^- data [14–18]. In such analyses a parametrization is chosen for the z -dependence of $H_{1q}^{\perp h}$, while the Gaussian ansatz is assumed for the p_T -dependence. These assumptions are then reflected on the dependence of the Collins analysing power on z and p_T . Furthermore, assuming isospin and charge conjugation invariance, the favoured spin-averaged FF $D_F = D_{1u}^{\pi^+} = D_{1d}^{\pi^-} = D_{1\bar{u}}^{\pi^-} = D_{1\bar{d}}^{\pi^+}$ and the unfavoured spin-averaged FF $D_U = D_{1u}^{\pi^-} = D_{1d}^{\pi^+} = D_{1\bar{u}}^{\pi^+} = D_{1\bar{d}}^{\pi^-}$ are introduced. Analogously, the favoured (H_F) and unfavoured (H_U) Collins FFs are defined. Using these definitions, one obtains the favoured (unfavoured) Collins analysing power a_p^F (a_p^U) by inserting H_F and D_F (H_U and D_U) in Eq. (18).

The string+ 3P_0 model, on the other hand, produces its own prediction for the Collins analysing power. This quantity was extensively studied in the previous works by the means of a standalone Monte Carlo implementation of the string+ 3P_0 model [21–23]. However, given the satisfactory description of the e^+e^- data achieved in Sec. IV, it is interesting to evaluate the resulting Collins analysing power and compare it with phenomenological analyses. After recalling the steps for calculating the Collins analysing power from simulated data in Sec. VA, we show the results and the comparison with phenomenological analyses in Sec. VB.

A. Calculation of the Collins analysing power from simulated data

The Collins analysing power $a_p^{q^\uparrow \rightarrow h+X}$ can be accessed in simulations of the fragmentation chain of a transversely polarized quark q^\uparrow . In the string+ 3P_0 model it consists in simulating the fragmentation of a string stretched between a $q^\uparrow \bar{q}$ pair where only q is transversely polarized and the fragmentation chain is evolved from q towards the \bar{q} side. Taking the transverse polarization of q with respect to the string axis to be \mathbf{S}_{qT} , the joint spin density matrix to be used in simulations is given by $\rho(q, \bar{q}) = \rho(q) \otimes 1^{\bar{q}}$, where the spin density matrix of q is $\rho(q) = (1^q + \boldsymbol{\sigma}^q \cdot \mathbf{S}_{qT})/2$. To simplify, we take q to be in the pure state with $\mathbf{S}_{qT} = \hat{\mathbf{y}}_q$ ($|\mathbf{S}_{qT}| = 1$).

The azimuthal distribution of the hadron h produced in the fragmentation of q^\uparrow is expected to be [2]

$$\frac{dN_h}{d\phi_C dz dp_T} \propto 1 + a_p^{q^\uparrow \rightarrow h+X}(z, p_T) |\mathbf{S}_{qT}| \sin \phi_C, \quad (19)$$

where the Collins angle ϕ_C is given by $\phi_C = \phi_{S_q} - \phi_h$. ϕ_{S_q} and ϕ_h are the azimuthal angle of \mathbf{S}_{qT} and the azimuthal angle of \mathbf{p}_T , respectively, evaluated in the QHF. The Collins analysing power is thus the amplitude of the $\sin \phi_C$ modulation. As can be deduced from Eq. (19), it can be calculated as $a_p^{q^\uparrow \rightarrow h+X}(z, p_T) = 2 \langle \sin \phi_C \rangle$ in a selected z or p_T interval.

To calculate the Collins analysing power we performed simulations of fragmentations of $u^\uparrow \bar{u}$ strings at the CMS energy $\sqrt{s} = 10.6$ GeV using the same free parameters as in Sec. IVA.

B. Comparison of the Collins analysing power with phenomenological analyses

As a preliminary step, we checked that the isospin and charge conjugation relations used to define the favoured and unfavoured FFs hold also in simulations. This is as expected because the isospin and charge conjugation symmetries are employed in PYTHIA to calculate the probabilities for projecting a given quark-antiquark pair onto a hadronic state.

Afterwards we evaluate a_p^F and a_p^U by looking at the distribution in Eq. (19) for, respectively, final state π^+ and π^- mesons. The result is shown as a function of z in Fig. 14. The top panel shows a_p^F as given by the string+ 3P_0 model (circles), while the bottom panel shows a_p^U (triangles). The favoured and unfavoured analysing powers have about the same size but opposite sign [21–23].

In the same figure are shown the favoured and unfavoured Collins analysing powers evaluated by using the Collins FFs extracted by different groups [15, 34, 35]. The same color-code is used for both a_p^F and a_p^U . The continuous line is the analysing power extracted in Ref. [15] (TS-TO15) using only the BELLE data on A_{12}^{UL}

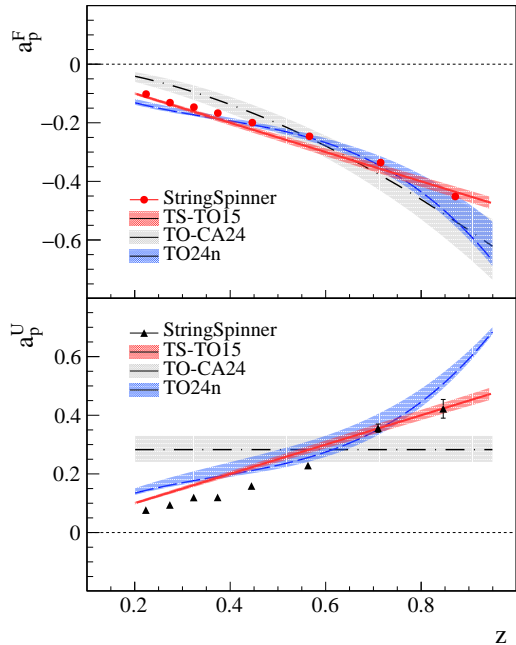


FIG. 14. Comparison between the Collins analysing power for favoured (circles) and unfavoured (triangles) fragmentation as obtained from the string+ 3P_0 model and the corresponding results from different phenomenological analyses (see text).

[3] and assuming the relation $a_p^F = -a_p^U$ ("scenario 2"). The enveloping red band represents a two standard deviations confidence interval (CL) evaluated by using the estimated uncertainty on the only free parameter of the a_p^F [15]. The gray band shows the 95% CL interval for the analysing power from the analysis performed in Ref. [34] (TO-CA24) using the SIDIS, e^+e^- and proton-proton data. The dashed-dotted line is the corresponding median value of the analysing power. The blue band shows the analysing power as obtained by a revisited TO-CA24 analysis (TO24n) [35] that in addition includes the recent Collins asymmetries in SIDIS with a deuteron target measured by COMPASS [12] and assumes a polynomial dependence on the Collins analysing power on z as in Ref. [36]. The band represents a two standard deviations CL interval, while the dashed line is the mean value of the analysing power.

As can be seen from the top panel in Fig. 14 the favoured Collins analysing power increases as a function of z , a feature common to the different extractions. The string+ 3P_0 result is remarkably similar to the TO24n extraction and not too far from a linear dependence on z as in the TS-TO15 extraction. Compared to the TO-CA24 extraction, the a_p^F results are similar for $z > 0.3$ but differ for smaller values. Concerning the unfavoured analysing power a_p^U , the string+ 3P_0 model predicts again a rising trend with z , as also obtained in TS-TO15 and TO-CA24.

A different result for a_p^U is obtained in the TO-CA24

extraction, where a constant expression for the analysing power as a function of z (i.e., same z -dependence for H_U and D_U) is found to be adequate for a satisfactory description of the data. This assumption has been successfully used also in previous analyses [14, 37]. The difference between the two results can be seen as an additional uncertainty on the knowledge of the unfavoured Collins FF as obtained from phenomenological analyses.

In this respect, models of polarized hadronization, such as the string+ 3P_0 model, can be used as a guide for the choice of the parametrization of the Collins FFs to be employed in the phenomenological analysis of SIDIS, e^+e^- and proton-proton data. In particular, the string+ 3P_0 model suggests a polynomial functional form for the z dependence of the favoured and unfavoured Collins analysing powers. It implements the fact that the information on the spin state of the fragmenting quark decays along the fragmentation chain and the memory of this state becomes negligible at small z .

VI. CONCLUSIONS

The string+ 3P_0 model of hadronization is implemented for the first time in the PYTHIA 8 event generator for the simulation of the e^+e^- annihilation to hadrons with quark spin effects. We use the recursive recipe for the simulation of the spin-dependent string fragmentation of a quark-antiquark pair with entangled spin states proposed recently in Ref. [26]. The actual implementation in PYTHIA is performed by developing further the **StringSpinner** package, which now can be applied to generate either polarized DIS events or e^+e^- events.

In this work, we used the new package to simulate e^+e^- annihilation events at the CMS energy $\sqrt{s} = 10.6$ GeV assuming the annihilation to occur by the exchange of a virtual photon. This corresponds to the kinematic configuration of the BELLE and BABAR experiments. The generated events are analyzed to calculate the Collins asymmetries for back-to-back hadrons in the e^+e^- CMS system by exploiting both the thrust axis method and the hadronic plane method. The simulated Collins asymmetries are compared to data from the BELLE and BABAR collaborations. A satisfactory comparison is found with the BELLE data for the both Collins asymmetries calculated by using the thrust axis method and the hadronic plane method. The comparison with the BABAR data is also satisfactory, with the exception of the A_{12} asymmetries for charged pions. The inconsistencies between the BABAR and the BELLE results for these asymmetries are, however, known.

Using the simulations, we also calculated the favoured and unfavoured Collins analysing powers predicted by the string+ 3P_0 model as a function of the fractional energy. The results were shown to be similar to those of phenomenological extractions that assume a non-constant dependence of the unfavoured analysing power on the fractional energy.

To conclude, considering the encouraging results obtained in this work, we believe that the string+ 3P_0 model is a sound model for the description of the quark-spin effects in hadronization and that it can be used for a systematical implementation of such effects in Monte Carlo event generators.

The `StringSpinner` code used in this paper will become available as a contributed module to `PYTHIA`, available from gitlab at gitlab.com/pythia8-contrib.

ACKNOWLEDGMENTS

The authors are grateful to Xavier Artru for the many enlightening discussions, to Isabella Garzia for clarifica-

tions on the BABAR data, and to Elena Boglione and Carlo Flore for useful discussions on the parametrizations of the Collins function and for providing the bands of the TO-CA24 and TO24n fits.

The work of A. K. is done in the context of the project “POLFRAG: Simulation of polarized quark fragmentation and application to the investigation of the nucleon structure”, CUP No. J97G22000510001, funded by the Italian Ministry of University and Research (MUR). A. K. acknowledges also support from the University of Trieste via the project “Simulazione delle correlazioni quantistiche in collisioni ad alta energia”, CUP No. J93C22001380002. L. L. was supported by the MC-netITN3 H2020 Marie Curie Initial Training Network, contract 722104. In addition L. L. is supported by Swedish Research Council contract 2020-04869.

-
- [1] J. C. Collins and D. E. Soper, Back-To-Back Jets in QCD, *Nucl. Phys. B* **193**, 381 (1981), [Erratum: *Nucl.Phys.B* 213, 545 (1983)].
- [2] J. C. Collins, Fragmentation of transversely polarized quarks probed in transverse momentum distributions, *Nucl. Phys. B* **396**, 161 (1993), [arXiv:hep-ph/9208213](https://arxiv.org/abs/hep-ph/9208213).
- [3] R. Seidl *et al.* (Belle), Measurement of Azimuthal Asymmetries in Inclusive Production of Hadron Pairs in e^+e^- Annihilation at $\sqrt{s} = 10.58$ -GeV, *Phys. Rev. D* **78**, 032011 (2008), [Erratum: *Phys.Rev.D* 86, 039905 (2012)], [arXiv:0805.2975](https://arxiv.org/abs/0805.2975) [hep-ex].
- [4] H. Li *et al.* (Belle), Azimuthal asymmetries of back-to-back $\pi^\pm - (\pi^0, \eta, \pi^\pm)$ pairs in e^+e^- annihilation, *Phys. Rev. D* **100**, 092008 (2019), [arXiv:1909.01857](https://arxiv.org/abs/1909.01857) [hep-ex].
- [5] J. P. Lees *et al.* (BaBar), Measurement of Collins asymmetries in inclusive production of charged pion pairs in e^+e^- annihilation at BABAR, *Phys. Rev. D* **90**, 052003 (2014), [arXiv:1309.5278](https://arxiv.org/abs/1309.5278) [hep-ex].
- [6] J. P. Lees *et al.* (BaBar), Collins asymmetries in inclusive charged KK and $K\pi$ pairs produced in e^+e^- annihilation, *Phys. Rev. D* **92**, 111101 (2015), [arXiv:1506.05864](https://arxiv.org/abs/1506.05864) [hep-ex].
- [7] M. Ablikim *et al.* (BESIII), Measurement of azimuthal asymmetries in inclusive charged dipion production in e^+e^- annihilations at $\sqrt{s} = 3.65$ GeV, *Phys. Rev. Lett.* **116**, 042001 (2016), [arXiv:1507.06824](https://arxiv.org/abs/1507.06824) [hep-ex].
- [8] A. Airapetian *et al.* (HERMES), Effects of transversity in deep-inelastic scattering by polarized protons, *Phys. Lett. B* **693**, 11 (2010), [arXiv:1006.4221](https://arxiv.org/abs/1006.4221) [hep-ex].
- [9] A. Airapetian *et al.* (HERMES), Azimuthal single- and double-spin asymmetries in semi-inclusive deep-inelastic lepton scattering by transversely polarized protons, *JHEP* **12**, 010, [arXiv:2007.07755](https://arxiv.org/abs/2007.07755) [hep-ex].
- [10] C. Adolph *et al.* (COMPASS), Collins and Sivers asymmetries in muonproduction of pions and kaons off transversely polarised protons, *Phys. Lett. B* **744**, 250 (2015), [arXiv:1408.4405](https://arxiv.org/abs/1408.4405) [hep-ex].
- [11] G. D. Alexeev *et al.*, Collins and Sivers transverse-spin asymmetries in inclusive muoproduction of ρ^0 mesons, *Phys. Lett. B* **843**, 137950 (2023), [arXiv:2211.00093](https://arxiv.org/abs/2211.00093) [hep-ex].
- [12] G. D. Alexeev *et al.* (COMPASS), High-statistics measurement of Collins and Sivers asymmetries for transversely polarised deuterons, (2023), [arXiv:2401.00309](https://arxiv.org/abs/2401.00309) [hep-ex].
- [13] X. Qian *et al.* (Jefferson Lab Hall A), Single Spin Asymmetries in Charged Pion Production from Semi-Inclusive Deep Inelastic Scattering on a Transversely Polarized ^3He Target, *Phys. Rev. Lett.* **107**, 072003 (2011), [arXiv:1106.0363](https://arxiv.org/abs/1106.0363) [nucl-ex].
- [14] M. Anselmino, M. Boglione, U. D’Alesio, J. O. Gonzalez Hernandez, S. Melis, F. Murgia, and A. Prokudin, Collins functions for pions from SIDIS and new e^+e^- data: a first glance at their transverse momentum dependence, *Phys. Rev. D* **92**, 114023 (2015), [arXiv:1510.05389](https://arxiv.org/abs/1510.05389) [hep-ph].
- [15] A. Martin, F. Bradamante, and V. Barone, Extracting the transversity distributions from single-hadron and di-hadron production, *Phys. Rev. D* **91**, 014034 (2015), [arXiv:1412.5946](https://arxiv.org/abs/1412.5946) [hep-ph].
- [16] M. Anselmino, M. Boglione, U. D’Alesio, J. O. Gonzalez Hernandez, S. Melis, F. Murgia, and A. Prokudin, Extracting the Kaon Collins function from e^+e^- hadron pair production data, *Phys. Rev. D* **93**, 034025 (2016), [arXiv:1512.02252](https://arxiv.org/abs/1512.02252) [hep-ph].
- [17] Z.-B. Kang, A. Prokudin, P. Sun, and F. Yuan, Extraction of quark transversity distribution and collins fragmentation functions with qcd evolution, *Phys. Rev. D* **93**, 014009 (2016).
- [18] J. Cammarota, L. Gamberg, Z.-B. Kang, J. A. Miller, D. Pitonyak, A. Prokudin, T. C. Rogers, and N. Sato (Jefferson Lab Angular Momentum), Origin of single transverse-spin asymmetries in high-energy collisions, *Phys. Rev. D* **102**, 054002 (2020), [arXiv:2002.08384](https://arxiv.org/abs/2002.08384) [hep-ph].
- [19] B. Andersson, G. Gustafson, G. Ingelman, and T. Sjostrand, Parton Fragmentation and String Dynamics, *Phys. Rept.* **97**, 31 (1983).
- [20] C. Bierlich *et al.*, A comprehensive guide to the physics and usage of PYTHIA 8.3, *SciPost Phys. Codebases* **8** (2022) [10.21468/SciPostPhysCodeb.8](https://arxiv.org/abs/2023.11601), [arXiv:2203.11601](https://arxiv.org/abs/2203.11601) [hep-ph].
- [21] A. Kerbizi, X. Artru, Z. Belghobsi, F. Bradamante, and A. Martin, Recursive model for the fragmentation

- of polarized quarks, *Phys. Rev. D* **97**, 074010 (2018), [arXiv:1802.00962 \[hep-ph\]](#).
- [22] A. Kerbizi, X. Artru, Z. Belghobsi, and A. Martin, Simplified recursive 3P_0 model for the fragmentation of polarized quarks, *Phys. Rev. D* **100**, 014003 (2019), [arXiv:1903.01736 \[hep-ph\]](#).
- [23] A. Kerbizi, X. Artru, and A. Martin, Production of vector mesons in the String+ 3P_0 model of polarized quark fragmentation, *Phys. Rev. D* **104**, 114038 (2021), [arXiv:2109.06124 \[hep-ph\]](#).
- [24] A. Kerbizi and L. Lönnblad, Extending StringSpinner to handle vector-meson spin, *Comput. Phys. Commun.* **292**, 108886 (2023), [arXiv:2305.05058 \[hep-ph\]](#).
- [25] A. Kerbizi and L. Lönnblad, StringSpinner - adding spin to the PYTHIA string fragmentation, *Comput. Phys. Commun.* **272**, 108234 (2022), [arXiv:2105.09730 \[hep-ph\]](#).
- [26] A. Kerbizi and X. Artru, String fragmentation of a quark pair with entangled spin states: Application to e^+e^- annihilation, *Phys. Rev. D* **109**, 054029 (2024), [arXiv:2312.14694 \[hep-ph\]](#).
- [27] U. D'Alesio, F. Murgia, and M. Zacccheddu, General helicity formalism for two-hadron production in e^+e^- annihilation within a TMD approach, *JHEP* **10**, 078, [arXiv:2108.05632 \[hep-ph\]](#).
- [28] K. Chen, G. R. Goldstein, R. L. Jaffe, and X.-D. Ji, Probing quark fragmentation functions for spin 1/2 baryon production in unpolarized e^+e^- annihilation, *Nucl. Phys. B* **445**, 380 (1995), [arXiv:hep-ph/9410337](#).
- [29] J. C. Collins, Spin Correlations in Monte Carlo Event Generators, *Nucl. Phys. B* **304**, 794 (1988).
- [30] I. G. Knowles, Spin Correlations in Parton - Parton Scattering, *Nucl. Phys. B* **310**, 571 (1988).
- [31] D. Boer, R. Jakob, and P. J. Mulders, Asymmetries in polarized hadron production in e^+e^- annihilation up to order $1/Q$, *Nucl. Phys. B* **504**, 345 (1997), [arXiv:hep-ph/9702281](#).
- [32] D. Boer, Angular dependences in inclusive two-hadron production at BELLE, *Nucl. Phys. B* **806**, 23 (2009), [arXiv:0804.2408 \[hep-ph\]](#).
- [33] M. Boglione and A. Simonelli, Full treatment of the thrust distribution in single inclusive $e^+e^- \rightarrow hX$ processes, *JHEP* **09**, 006, [arXiv:2306.02937 \[hep-ph\]](#).
- [34] M. Boglione, U. D'Alesio, C. Flore, J. O. Gonzalez-Hernandez, F. Murgia, and A. Prokudin, Simultaneous reweighting of Transverse Momentum Dependent distributions, *Phys. Lett. B* **854**, 138712 (2024), [arXiv:2402.12322 \[hep-ph\]](#).
- [35] M. Boglione and C. Flore, Private communication.
- [36] M. Anselmino, M. Boglione, U. D'Alesio, S. Melis, F. Murgia, and A. Prokudin, Simultaneous extraction of transversity and Collins functions from new SIDIS and e^+e^- data, *Phys. Rev. D* **87**, 094019 (2013), [arXiv:1303.3822 \[hep-ph\]](#).
- [37] U. D'Alesio, C. Flore, and A. Prokudin, Role of the Soffer bound in determination of transversity and the tensor charge, *Phys. Lett. B* **803**, 135347 (2020), [arXiv:2001.01573 \[hep-ph\]](#).